

# The Impact of the Temperature Sensitivity of Ecosystem Respiration on the Climate-Carbon Cycle Feedback Strength

Forrest M. Hoffman<sup>1,2</sup> (forrest@climatemodeling.org) and James T. Randerson<sup>2</sup> (jranders@uci.edu)

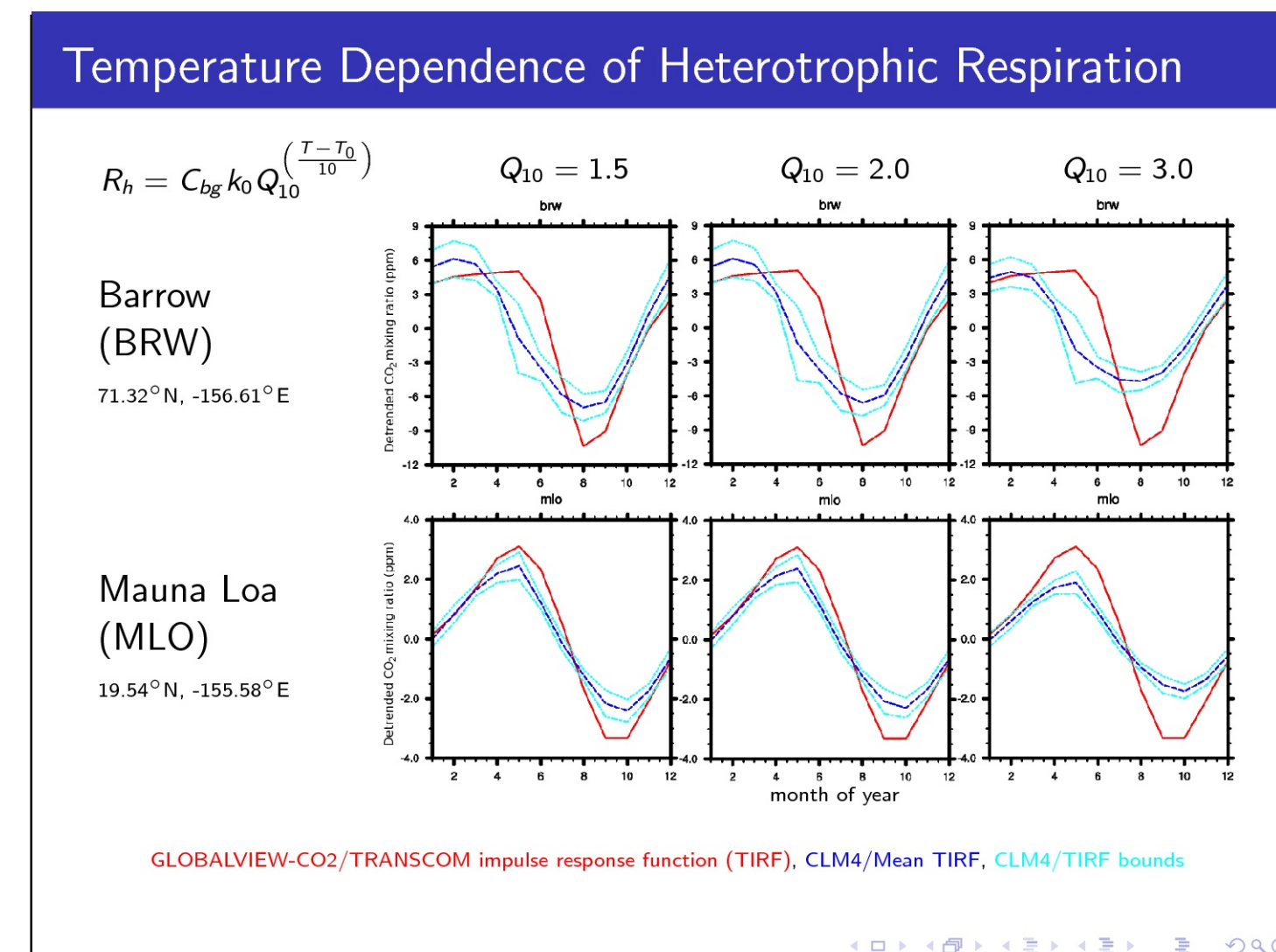
<sup>1</sup>Oak Ridge National Laboratory (ORNL) and <sup>2</sup>University of California-Irvine (UCI)

## Introduction

Rapidly increasing atmospheric carbon dioxide concentrations are altering the Earth's climate. The anthropogenic perturbation of the global carbon cycle is expected to induce feedbacks on global climate and future CO<sub>2</sub> concentrations. However, these feedbacks are poorly constrained and potentially large. Prediction of these feedbacks using Earth System Models (ESMs) requires knowledge of mechanisms connecting carbon and nutrients in the biosphere with the climate system. In order to reduce the range of uncertainty in climate predictions, model representation of feedbacks must be improved through comparisons with contemporary observations. The climate sensitivity of land carbon storage ( $\gamma_{land}$ ) varied by a factor of almost nine in the 11 C<sup>4</sup>MIP models (Friedlingstein *et al.*, 2006), suggesting a large uncertainty in ecosystem responses to climate change. The temperature sensitivity of terrestrial ecosystem respiration ( $Q_{10}$ ), a significant component of  $\gamma_{land}$ , was recently reported to be independent of mean annual temperature, constant across biomes, and confined to values around  $1.4 \pm 0.1$  based on observations from 60 FLUXNET sites, suggesting a weaker climate-carbon cycle than projected by most models (Mahecha *et al.*, 2010).

## Temperature Dependence of Heterotrophic Respiration ( $R_h$ )

In many biogeochemistry models, the  $Q_{10}$  factor controls the dependence of heterotrophic respiration on temperature (see equation below). Values of  $Q_{10}$  that are too large over-emphasize this temperature dependence and result in stronger respiration in mid-summer, producing a weakened seasonal cycle of CO<sub>2</sub>.

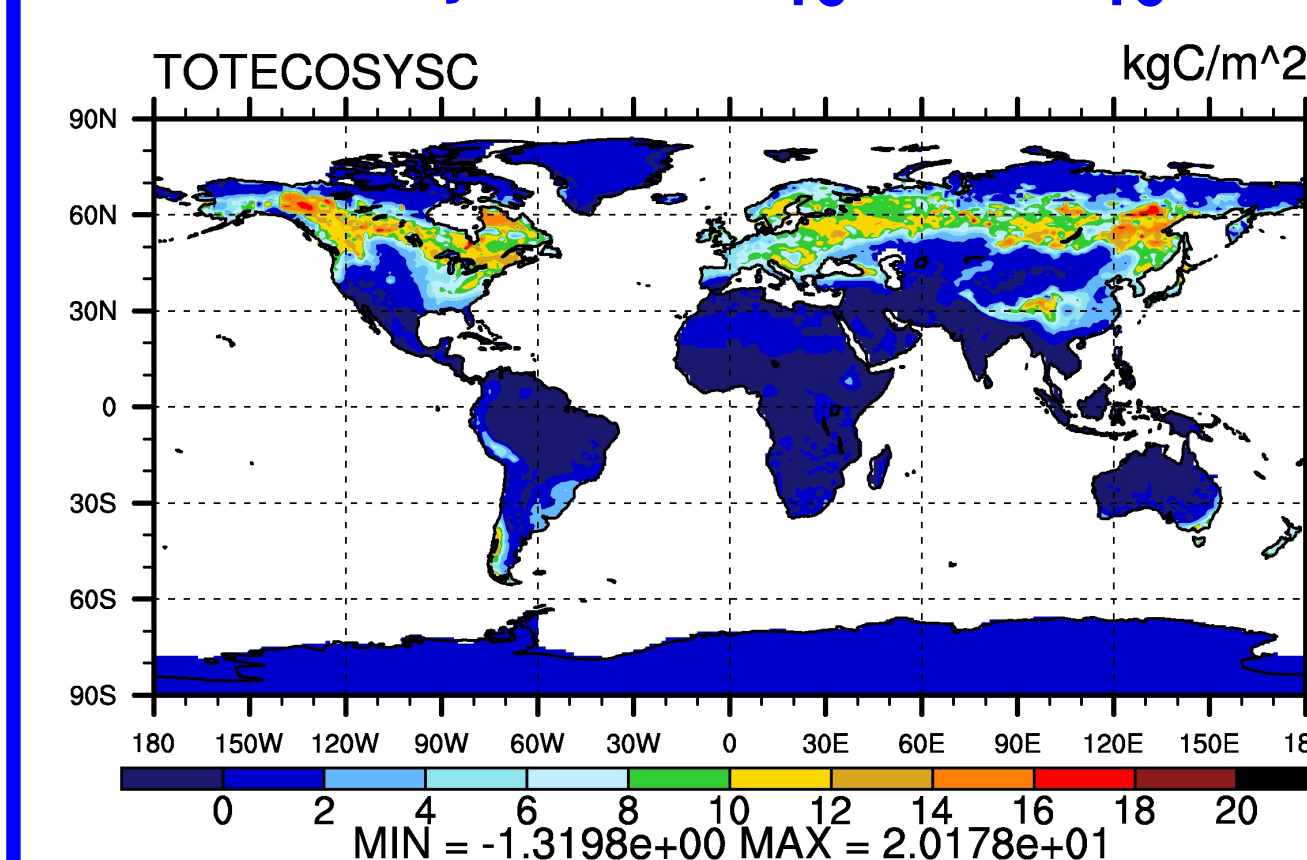


As a result, the observed annual cycle of CO<sub>2</sub> can be used to constrain the temperature dependence of respiration in ecosystems models.

This constraint was used to tune the Community Land Model (CLM4) based on the Carbon-Land Model Intercomparison Project (C-LAMP) metric for the annual cycle of CO<sub>2</sub>. See:

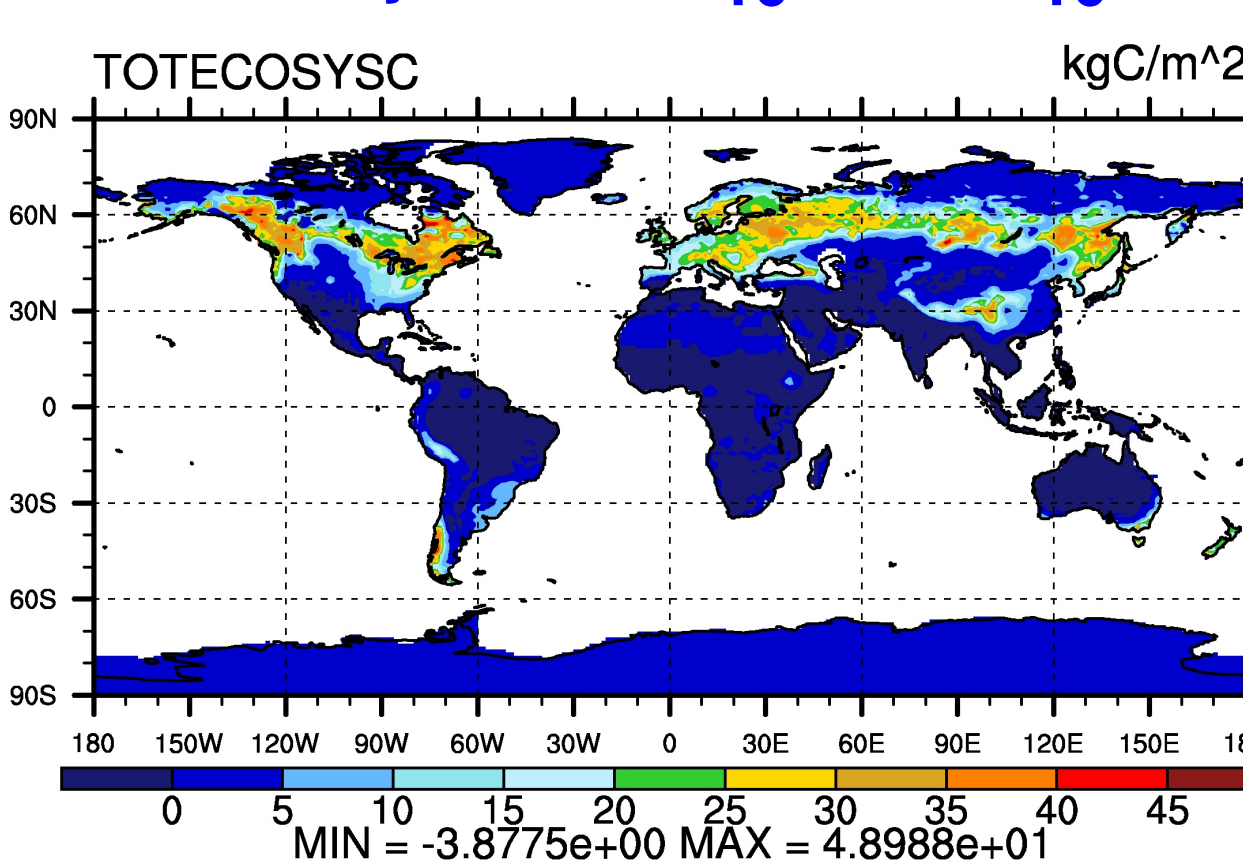
Randerson, James T., Forrest M. Hoffman, Peter E. Thornton, Natalie M. Mahowald, Keith Lindsay, Yen-Huei Lee, Cynthia D. Nevison, Scott C. Doney, Gordon Bonan, Reto Stöckli, Curtis Covey, Steven W. Running, and Inez Y. Fung. September 2009. "Systematic Assessment of Terrestrial Biogeochemistry in Coupled Climate-Carbon Models." *Global Change Biology*, 15(9):2462–2484. doi:10.1111/j.1365-2486.2009.01912.x.

Total Ecosystem C:  $Q_{10}=2.0 - Q_{10}=1.5$



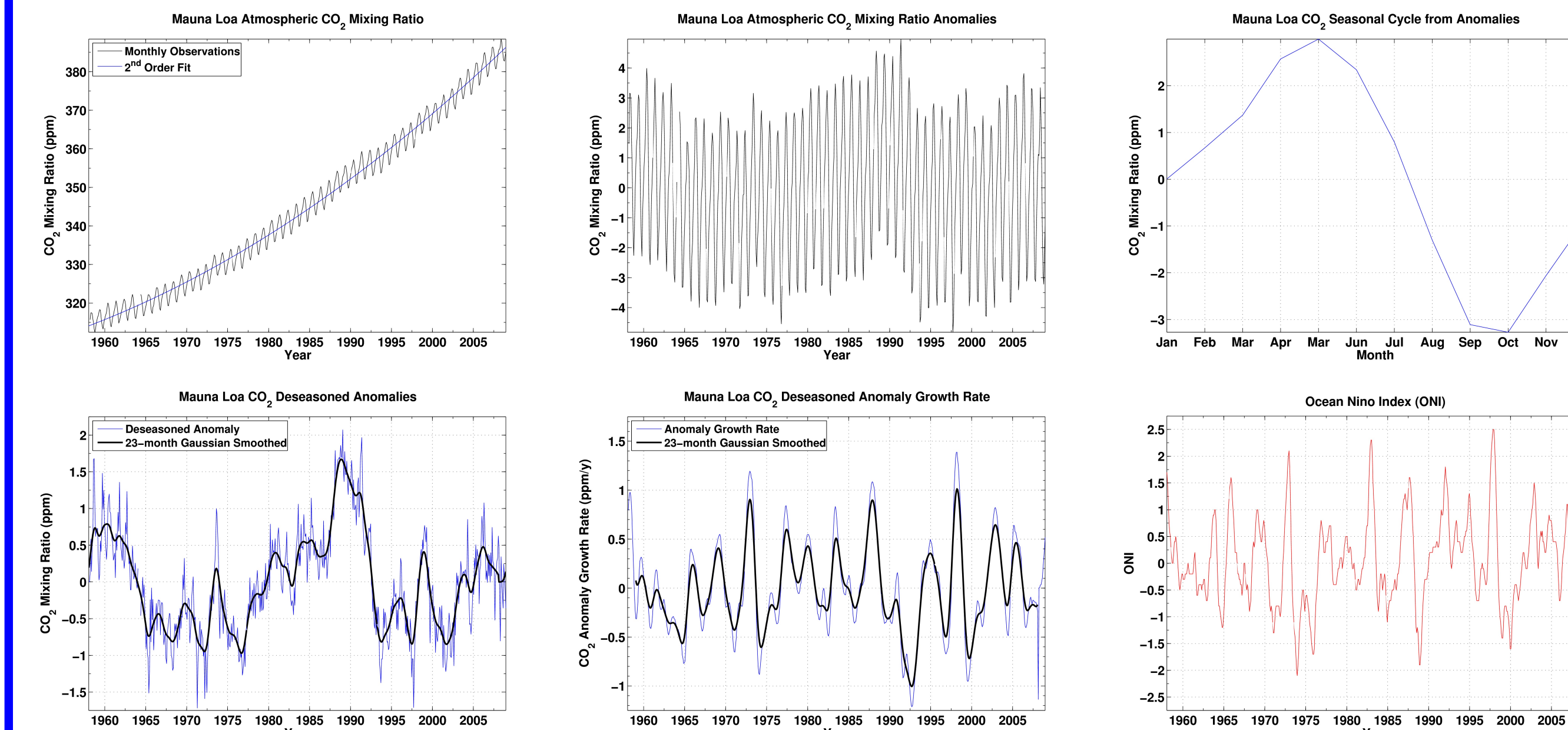
Higher  $Q_{10}$  values increase summertime heterotrophic respiration, resulting in higher rates of nitrogen mineralization and primary production (particularly at boreal latitudes), leaving more carbon in the ecosystem at equilibrium. Note the different plot scales.

Total Ecosystem C:  $Q_{10}=3.0 - Q_{10}=1.5$

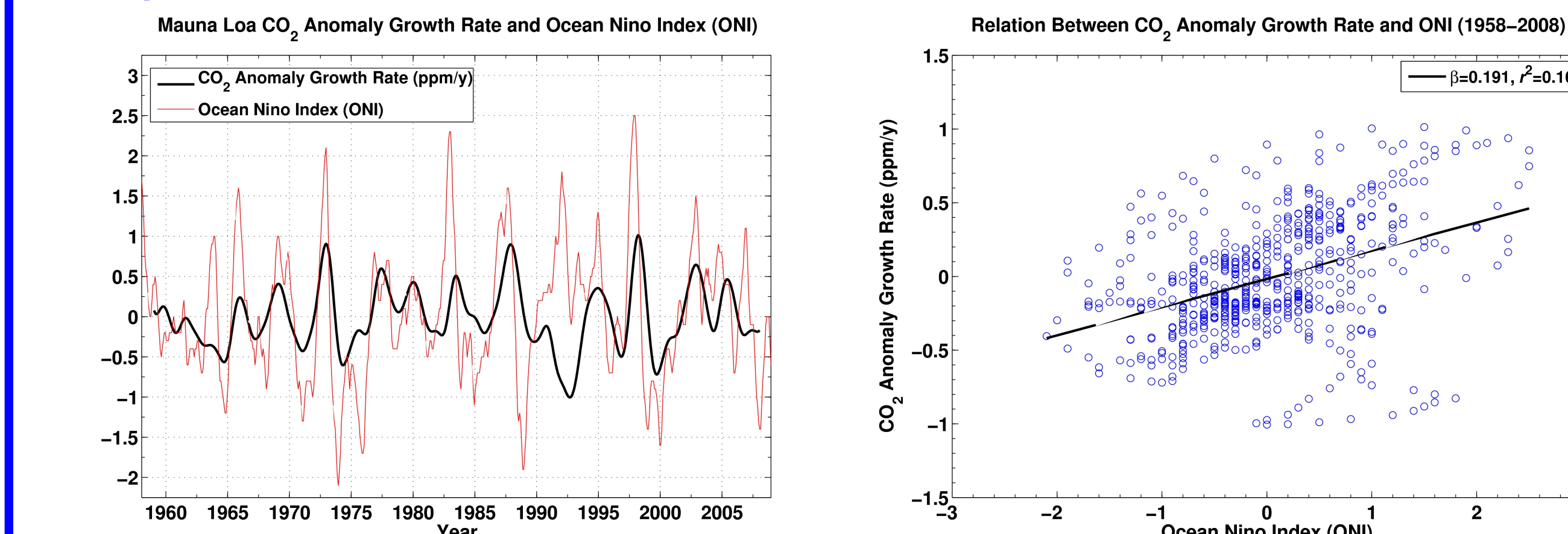


## Atmospheric CO<sub>2</sub> Dependence on El Niño

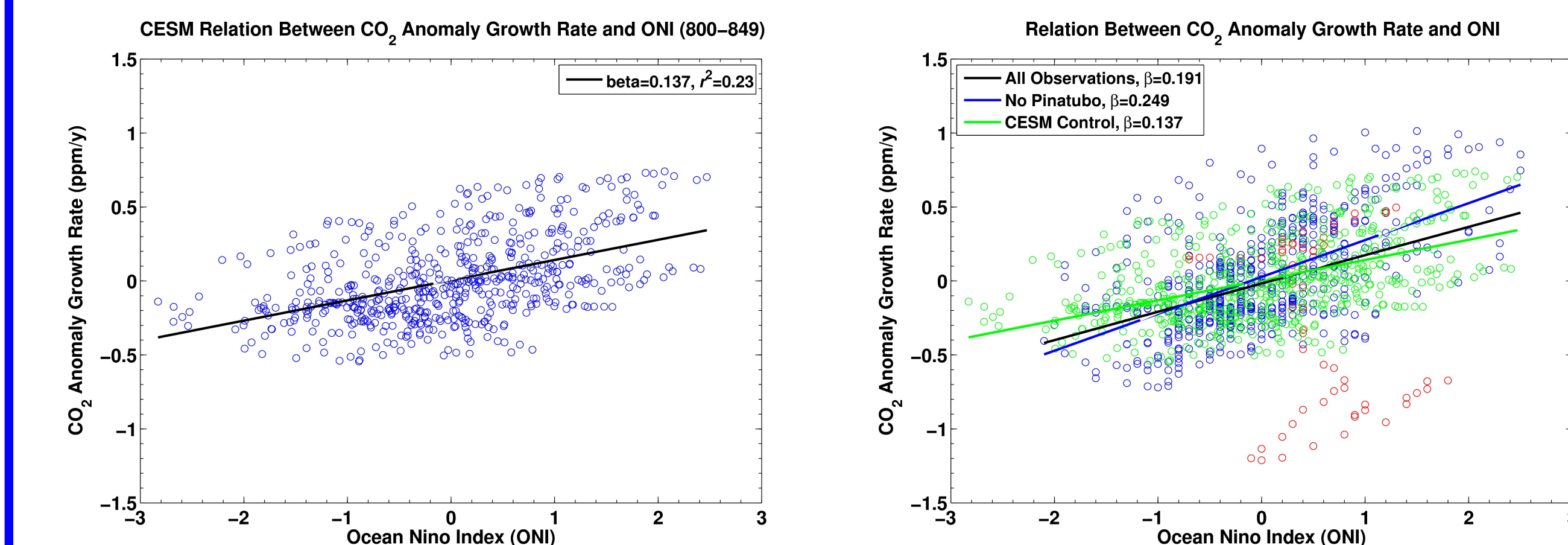
Hypothesis: The relationship between El Niño-Southern Oscillation (ENSO) and observed CO<sub>2</sub> anomalies at Mauna Loa may be exploited to evaluate ocean and terrestrial model responses over interannual to decadal time scales. The shutdown of ocean CO<sub>2</sub> out-gassing described by Keeling and Revelle (1985) is more than compensated for by plant deaths and forest fires due to El Niño-induced drought.



A second order linear fit is applied to the Keeling Curve of Mauna Loa CO<sub>2</sub> mixing ratio (panel 1) in order to remove the increasing trend, revealing the anomalies (panel 2). From these anomalies, a mean annual cycle of CO<sub>2</sub> is extracted (panel 3) and this cycle is removed from the anomalies, which are filtered by a 23-month Gaussian smoothing (panel 4). The filtered deseasoned anomalies are then used to calculate an anomaly growth rate, which is also filtered (panel 5). This filtered deseasoned anomaly growth rate of the monthly Mauna Loa CO<sub>2</sub> record can be compared to the Ocean Niño Index (ONI; panel 6).



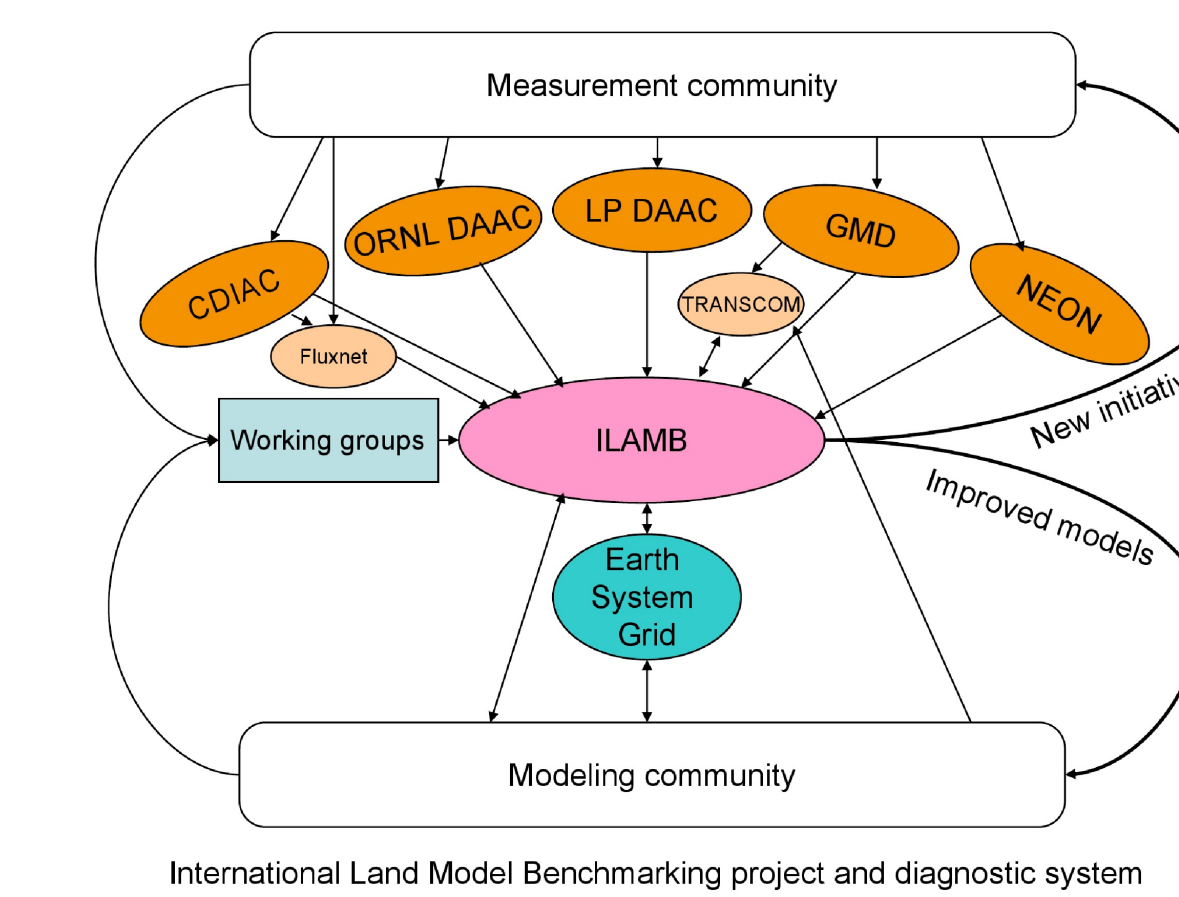
The atmospheric CO<sub>2</sub> anomaly growth rate appears to be strongly correlated with ONI except during periods of large volcanic eruptions (left). The largest of these in the record is the eruption of Mt. Pinatubo in June 1991. This relationship can be seen in the scatter plot at right.



The same relationship was extracted from a Community Earth System Model (CESM) control simulation (left). In the plot at right, the model relationship fit is plotted against that from observations with and without including the Mt. Pinatubo eruption period. Observations are shown in blue, model results are shown in green, and the observations from the Mt. Pinatubo period (1991–1993) are shown in red. From this plot, we can see that the CESM El Niño is a bit strong and that the 1991 to 1993 points from the Mt. Pinatubo period deviate significantly from the main body of the observations. The slope from the CESM control run is reasonably close to that of all the observations. An analysis such as this may prove useful in constraining models and in providing a model performance benchmark for coupled Earth System Models.

## International Land Model Benchmarking (ILAMB) Project

The ILAMB Project is designed to develop model evaluation benchmarks agreed upon by the larger international research community. A benchmark is a quantitative test of model function, for which uncertainties in observations can be quantified. Acceptable performance on benchmarks is a necessary but not sufficient condition for a fully functioning model. An effective benchmark is one that draws upon a broad set of independent observations to evaluate model performance on multiple temporal and spatial scales.



ILAMB will develop an extensible open source model diagnostics package that implements benchmarks for community use. By using the wide variety of measurements made, collected, and distributed by researchers and data centers, ILAMB will identify improvements for models as well as new kinds of measurements. ILAMB model output will be distributed via the Earth System Grid (ESG), and model diagnostics will be available on the Web for use by the wider scientific community.

## ILAMB Community Meeting

The First ILAMB Meeting, held in January, consisted of about 45 researchers. Participants agreed upon an initial set of benchmarks, cost functions, and observational data sets for evaluating global models. An approach for developing ILAMB software and applying benchmarks to TRENDY and CMIP5 results was discussed.



## Initial ILAMB Benchmarks and Datasets

	Annual Mean	Seasonal Cycle	Interannual Variability	Trend	Data Source
<b>Atmospheric CO<sub>2</sub></b>					
Flask/conc. + transport	✓	✓	✓	✓	NOAA, SIO, CSIRO
TCCON + transport	✓	✓	✓	✓	Caltech
<b>Fluxnet</b>					
GPP: NEE, TER, L_E, H, RN	✓	✓	✓	✓	Fluxus, MAST-DC
Gridded: GPP	✓	✓	?		MPI-BGC
<b>Hydrology/Energy</b>					
river flow	✓		✓		GRDC, Dai, GFDL
global runoff/ocean balance	✓				Syed/Famiglietti
albedo (multi-band)	✓	✓	✓		MODIS, CERES
soil moisture	✓	✓	✓		de Jeu, SMAP
column water	✓	✓	✓		GRACE
snow cover	✓	✓	✓	✓	AVHRR, GlobSnow
snow depth/SWE	✓	✓	✓	✓	CMC (N. America)
T <sub>air</sub> & P	✓	✓	✓	✓	CRU, GPCP and TRMM
Gridded: L_E, H	✓	✓	✓	✓	MPI-BGC, dedicated ET
<b>Ecosystem Processes &amp; State</b>					
soil C, N	✓				HWSD, MPL-BGC
litter C, N	✓				LIDET
soil respiration	✓	✓	✓	✓	Bond-Lamberty
FAPAR	✓	✓	✓		MODIS, SeaWiFS
biomass & change	✓	✓	✓	✓	Saatchi, Pan, Blackard
canopy height	✓				Lefsky, Fisher
NPP	✓				EMDL, Layssaert
<b>Vegetation Dynamics</b>					
fire — burned area	✓	✓	✓		GFED3
wood harvest	✓			✓	Hurt
land cover	✓				MODIS PFT fraction

The initial set of benchmarks and available observational data sets identified at the ILAMB meeting is shown in this table.

Depending upon the type of measurements available, the annual mean, seasonal cycle, interannual variability, and long-term trend of the model results will be assessed.

Observational data sets span scales from site/point *in situ* measurements to global remote sensing observations.



Acknowledgements: Research partially sponsored by the Climate and Environmental Sciences Division (CESD) of the Office of Biological and Environmental Research (OBER) within the U.S. Department of Energy's Office of Science (SC). This research used resources of the National Center for Computational Sciences (NCCS) at Oak Ridge National Laboratory (ORNL), which is managed by UT-Battelle, LLC, for the U.S. Department of Energy under Contract No. DE-AC05-00OR22725.